Ultrasonics Sonochemistry 21 (2014) 136–141

Contents lists available at ScienceDirect

Ultrasonics Sonochemistry

journal homepage: www.elsevier.com/locate/ultson

# Fabrication and sonocatalytic property of $AgPO_3$ microsphere

Peizhi He [a], Limin Song [a,*], Xiaoqing Wu [b,*], Haifeng Tian [a], Qingwu Wei [a], Jiayi Ye [a], Longguang Zhang [a], Yuanyuan Cui [a], Yanbing Wang [a]

[a] College of Environment and Chemical Engineering & State Key Laboratory of Hollow-Fiber Membrane Materials and Membrane Processes, Tianjin Polytechnic University, Tianjin 300387, PR China

[b] Institute of Composite Materials & Ministry of Education Key Laboratory of Advanced Textile Composite Materials, Tianjin Polytechnic University, Tianjin 300387, PR China

ARTICLE INFO

*Article history:*
Received 22 November 2012
Received in revised form 23 July 2013
Accepted 29 July 2013
Available online 7 August 2013

*Keywords:*
$AgPO_3$ microspheres
Sonodegradation
Rhodamine B

ABSTRACT

$AgPO_3$ microspheres were prepared by a simple hydrothermal method. The $AgPO_3$ microspheres were characterized by X-ray powder diffraction (XRD), scanning electronic microscopy (SEM), Brunauer–Emmett–Teller (BET), UV–vis absorption spectroscopy (UV–vis), and photoluminescence (PL) measurement. SEM reveals that the $AgPO_3$ microspheres were constructed by the accumulation of small particles. The as-prepared $AgPO_3$ microspheres sonocatalytically degraded Rhodamine B (RhB) excellently under ultrasonic irradiation. The sonocatalytic ability results from the $^{\cdot}OH$ radicals induced by $AgPO_3$ microspheres under ultrasonic irradiation. The effects of other conditions on ultrasonic activity were also investigated. The content of $^{\cdot}OH$ radicals in the reaction system was determined to further verify the above conclusions.

## 1. Introduction

It is well known that cavitation can be induced in the solution under ultrasonic irradiation, which undergoes nucleation, growth/expansion and collapse of microbubbles. The sudden collapse of the microbubbles results in high local temperature (5000 K) and pressure (1000 atm), which thermally dissociate water into $^{\cdot}OH$ radicals that can oxidize organic dyes. Therefore, organic dyes can be oxidized under ultrasonic irradiation.

It has been previously reported several outstanding metal oxide sonocatalysts, such as $TiO_2$, ZnO and etc. [1–9]. In the study, $AgPO_3$ microspheres were prepared by a simple hydrothermal method. To the best of our knowledge, $AgPO_3$ microspheres have never been reported. The structure and property of the as-obtained $AgPO_3$ microspheres were studied in detail. Meanwhile, their sonodegradation abilities for dyes were studied thoroughly. The kinetic data were also calculated and discussed based on the measurement of sonodegradation activity.

## 2. Experimental

### 2.1. Synthesis of samples

0.69 g $AgNO_3$ was dissolved in 20 mL of deioned water. 0.42 g of $(NaPO_3)_6$ was dissolved in 40 mL deioned water. The $(AgPO_3)_6$ solution was dropwise added into the $AgNO_3$ solution under continuous stiring. The above mixture was transferred into a 60 mL stainless teflonlined autoclave and heated at 80 °C for 6 h. The resulting precipitate was collected, centrifuged, and washed with deioned water three times. The as-obtained precipitate was dried at 60 °C for 6 h in a vacuum oven.

### 2.2. Characterization of samples

X-ray diffraction (XRD) was recorded on a Rigaku D/max 2500 diffractometer. crystallite size (ds) was calculated from the strongest diffraction of $AgPO_3$ microspheres. $N_2$ adsorption was carried out on a Quantachrome NOVA 2200e at 77 K, from which the BET specific surface area (Asp) was calculated. Scanning electron microscope (SEM) measurement was performed on a Hitachi S-4800. The UV–vis absorption spectroscopy was measured on a Shimadzu UV-2550PC spectrometer using $BaSO_4$ as a reference. The photoluminescence spectra (PL) of samples were done on a Shimadzu RF-5301 (excitated at 325 nm) photoluminescence analyzer.

### 2.3. Activity measurement

All experiments were carried out in a KQ-100 ultrasonics apparatus (Kunshan apparatus company, China). Ultrasonic frequency and output power are 40 kHz and 0–100 W, respectively. In a typical experiment, 0.1 g of $AgPO_3$ microspheres was dispersed in 100 ml (1 g/L) of RhB solution (10 mg/L). The mixture was stirred in the dark for 30 min to allow the physical adsorption of RhB

---

* Corresponding authors. Tel./fax: +86 22 83955458.
*E-mail addresses:* songlmnk@sohu.com (L. Song), wuxiaoqing@yahoo.cn (X. Wu).

1350-4177/$ - see front matter
http://dx.doi.org/10.1016/j.ultsonch.2013.07.017

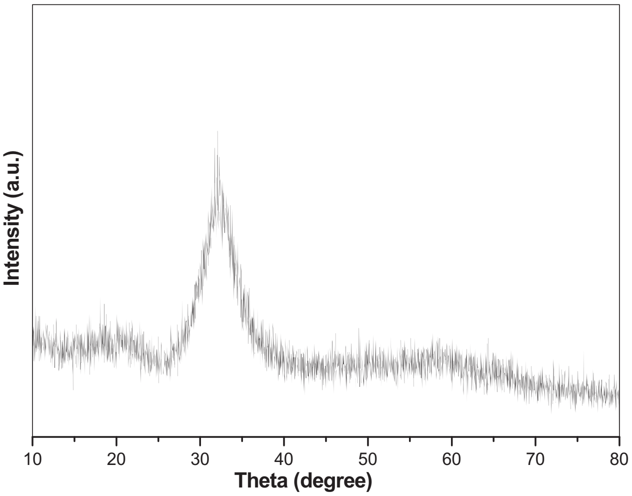

**Fig. 1.** X-ray diffraction patterns of the resulting $AgPO_3$ microspheres.

molecules on $AgPO_3$ microspheres reaching the equilibrium. Subsequently, the mixture was bubbled by an air diffuser under ultrasonic irradiation, and the sonocatalytic degradation measurement began. At the intervals of 30 min, 5 mL of the mixture was collected and centrifuged to remove the $AgPO_3$ microspheres. Residual solution was measured on a UV spectrometer using 554 nm light.

### 2.4. Hydroxyl radicals measurement

The measurement of $^{\cdot}OH$ radicals was as follows: 5 mg of $AgPO_3$ microspheres was dispersed in a 80 mL aqueous solution of 3 mmol/L terephthalic acid and 0.01 mol/L NaOH in a reactor under ultrasonic irradiation at room temperature. At the intervals of 10 min, 3 mL of the mixture was collected and centrifuged to remove the $AgPO_3$ microspheres. PL spectra of the 2-hydroxyterephthalic acid formed by the reaction between terephthalic acid and songenerated $^{\cdot}OH$ radicals were measured on a PL spectrometer using 325 nm excitation light.

Terephthalic acid reacts with hydroxyl radicals to produce 2-hydroxyterephthalic acid in alkaline conditions. 2-hydroxyterephthalic acid has a strong fluorescence emission at 425 nm. Therefore, 2-hydroxyterephthalic acid has a greater concentration if the songenerated $^{\cdot}OH$ radicals in the solution increase. The fluorescence emission peak at 425 nm becomes stronger. The songenerated $^{\cdot}OH$ radicals in solution can be determined by the fluorescence peak intensity of 425 nm.

## 3. Results and discussion

### 3.1. Characterization of photcatalysts

XRD patterns of the as-prepared sample are shown in Fig. 1. Only one broad diffraction peak at 31.695° is observed, which can be assigned to the strongest peak of $AgPO_3$ (JCPDS file 11-0640). The JCPDS data of $AgPO_3$, including the crystal system

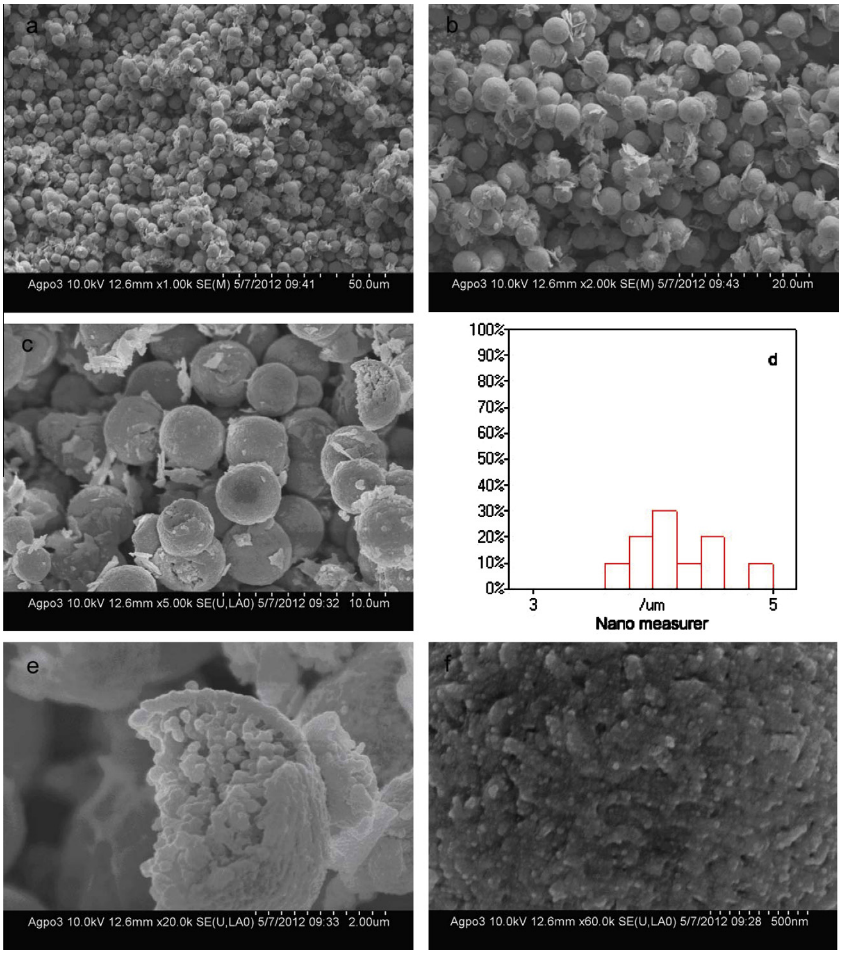

**Fig. 2.** (a–c) and (e and f) SEM image; (d) particle mean size distribution of $AgPO_3$ microspheres.

**Table 1**
Physical parameters of $AgPO_3$.

| Sample | $d_s$ (nm) | $S_{BET}$ ($m^2/g$) | $V_p$ ($cm^3/g$) | $d_p$ (nm) |
|---|---|---|---|---|
| $AgPO_3$ | 58 | 0.414 | 0.001 | 3.444 |

Definitions: $d_s$, crystal size; $S_{BET}$, BET surface area; $V_p$, total pore volume; $d_p$, BJH average pore size.

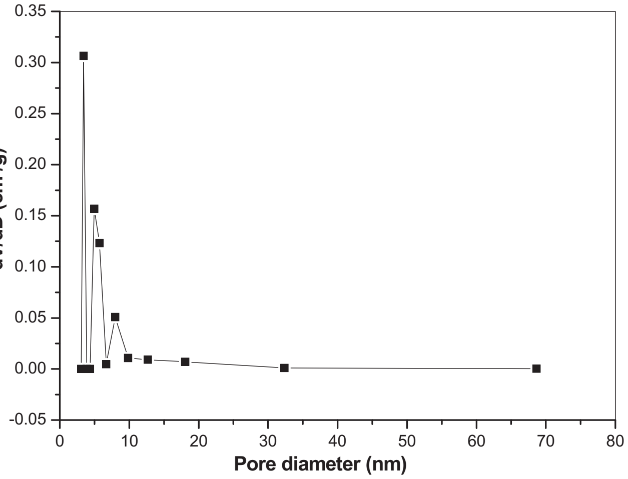

**Fig. 3.** The pore-size distribution of $AgPO_3$ microspheres.

and lattice constants, have not been updated. Therefore, the JCPDS data were not further compared. The top of this broad $AgPO_3$ diffraction peak is quite sharp, revealing that the sample is crystalline. The highly broad diffraction peak indicates that the sample consists of tiny crystallites. The mean crystallite size (ds) was calculated as 58 nm by the scherrer equation on the basis of the strongest peak of $AgPO_3$.

The microstructures of the as-prepared sample were then examined by the microscope. The morphology of the as-obtained particles shown in Fig. 2a–c can be described as $AgPO_3$ microspheres. The particle sizes in Fig. 2d range from 3.67 to 4.93 μm, and the mean particle diameter is 4.23 μm. The difference between the maximal and minimal sizes of the particles is about 1.2 μm. Many tiny particles are discerned inside the microsphere (Fig. 2e), which contributes to the only one broad and sharp diffraction peak in the XRD pattern. The magnified image (Fig. 2f) shows many tiny pores on the surface of the microsphere. However, those tiny pores do not offer large specific surface area for $AgPO_3$ microspheres (Table 1).

$N_2$ adsorption–desorption of the $AgPO_3$ microspheres (Fig. 3) indicates a narrower mesopore size distribution of $AgPO_3$ particles at 4.7 and 7.8 nm. According to Fig. 2e and f, the small and the large mesopores in the $AgPO_3$ microspheres may be assigned to intra-aggregated pores and the pores among inter-aggregated particles. As shown in Table 1, the specific surface area, the total pore

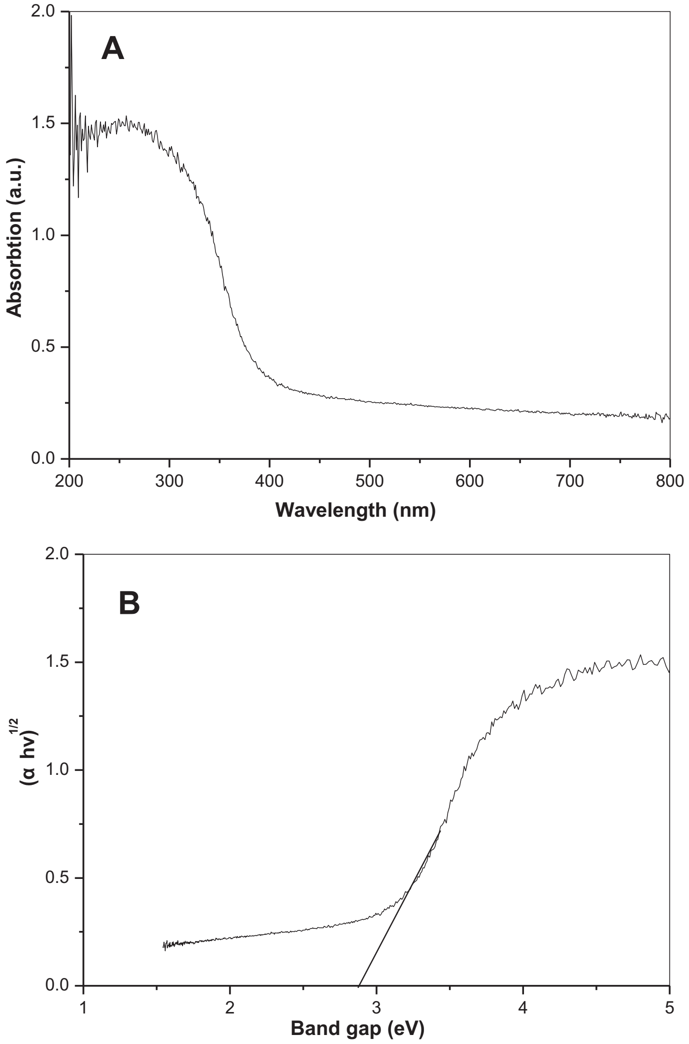

**Fig. 4.** UV–vis absorption spectra of the as-synthesized $AgPO_3$ microspheres.

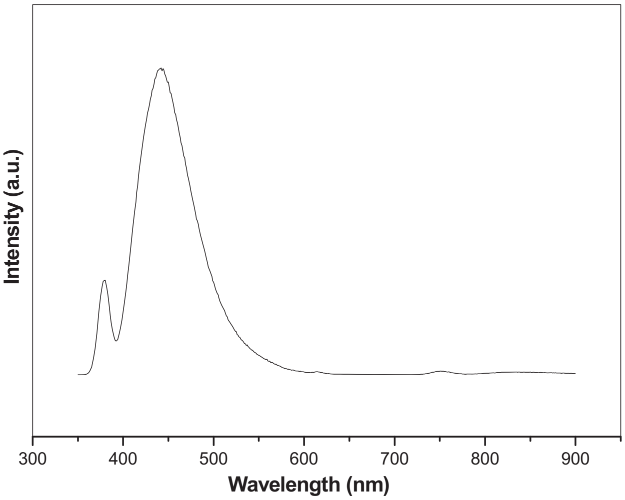

**Fig. 5.** PL spectra of the as-synthesized $AgPO_3$ microspheres.

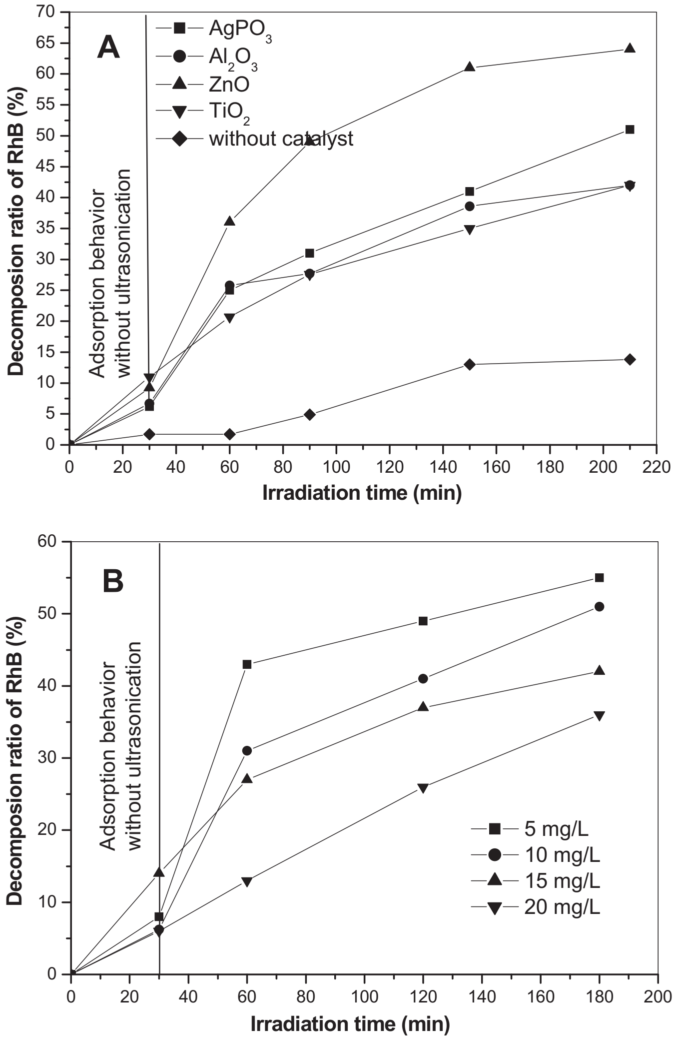

**Fig. 6.** (A) The dependence of sonocatalytic activity on different catalysts; (B) The dependence of sonocatalytic activity on the original concentration of RhB.

volume and the average pore size of the $AgPO_3$ microspheres are 0.414 $m^2/g$, 0.001 $cm^3/g$ and 3.414 nm, respectively.

Fig. 4A shows the UV–vis absorption spectra of the $AgPO_3$ microspheres, which exhibits an absorption maximum in the range of 200–400 nm. However, they absorb more weakly in the visible light region. The onset of absorption is estimated to be about 2.88 eV (Fig. 4B). The above results imply that the as-synthesized $AgPO_3$ microspheres are sensitive to ultraviolet and visible light.

Fig. 5 shows the PL spectrum of the $AgPO_3$ microspheres. There are two emission bands upon excitation at 325 nm. The strongest peak centered at about 442 nm is assigned to the band–band transition. The shoulder peak at approximately 380 nm is attributed to the oxygen vacancies.

### *3.2. Sonocatalytic activity and mechanism of $AgPO_3$ microspheres*

Sonocatalytic activity of the $AgPO_3$ microspheres is shown in Fig. 6A. The concentration of catalyst and RhB in solution is 1 g/L and 10 mg/L, respectively. The mixture of $AgPO_3$ and RhB solution is stirred for 30 min to reach the adsorption equilibrium. The adsorption amount is only 6.2%, indicated that it cannot affect the sonocatalytic activity of the $AgPO_3$ microspheres obviously in Fig. 6A. It is very clear that the sonodegradation ratio is 51% after 180 min in Fig. 6A. In addition, the blank experiment without catalyst has been carried out in Fig. 6A. The decomposition ratio by oneself is 13.9% after 180 min under ultrasonic irradiation. The result shows the RhB molecules can be degraded over $AgPO_3$ microspheres under ultrasonic irradiation. In order to discuss the role of $AgPO_3$ particles, sonocatalytic activity of $TiO_2$, ZnO, and $Al_2O_3$ powder (commercial analytical grade, 99%) under the same experimental condition has been researched in Fig. 6A. Their adsorption amount is 11%, 9.2% and 6.7% after 30 min, respectively. Fig. 6A shows that their sonodegradation ratio is 42%, 64% and 42%, respectively. In comparison with the as-prepared $AgPO_3$ microspheres, the order of their decomposition ratio is $ZnO > AgPO_3 > TiO_2 > Al_2O_3$. The result exhibits that the as-prepared $AgPO_3$ microspheres show a good role in the sonodegradation of organic dyes.

The dependence of sonocatalytic activity on the original concentration of RhB over the $AgPO_3$ microspheres (1 g/L) has been shown in Fig. 6B. Initial RhB concentrations are from 5 to 20 mg/L. Adsorption behavior of RhB on $AgPO_3$ microspheres has been shown in Fig 6B for different initial concentration of RhB. Their adsorption amount from 5 to 20 mg/L is 8%, 6.2%, 14% and 6% after 30 min, respectively. The adsorption amount is the largest for 15 mg/L RhB solution. The optimal sonodegradation activity was obtained in the presence of 5 mg/L RhB solution. Besides, the sonodegradation efficiency decreased with increasing concentration of RhB, suggesting that the sonodegradation rate depends on the concentration of RhB. In our experimental system, the high concentrations of organic molecules and the small opportunities that they encounter ·OH radicals produced by ultrasound mainly account for the reduced sonodegradation activity. Furthermore, the ·OH radicals concentration was measured within 60 min to investigate the sonocatalytic mechanism of the $AgPO_3$ microspheres [10].

Fig. 7 exhibits the dependence of the PL spectrum of terephthalic acid solution on irradiation time. The PL intensity at 425 nm gradually rises with increasing irradiation time in the presence of $AgPO_3$ (Fig. 7A). Therefore, the sonodegradation activity of the $AgPO_3$ microspheres also increases because their oxidation capacity results from ·OH radicals. The result is consistent with the activity of sonodegradation over $AgPO_3$ microspheres (Fig. 6A). In order to investigate the sonocatalytic mechanism of the $AgPO_3$ microspheres, ·OH radical contents are measured under different experimental conditions (Fig. 7B–D). Fig. 7B shows water without $AgPO_3$ microspheres can also produce a small amount of ·OH radicals under ultrasonic irradiation. However, the production

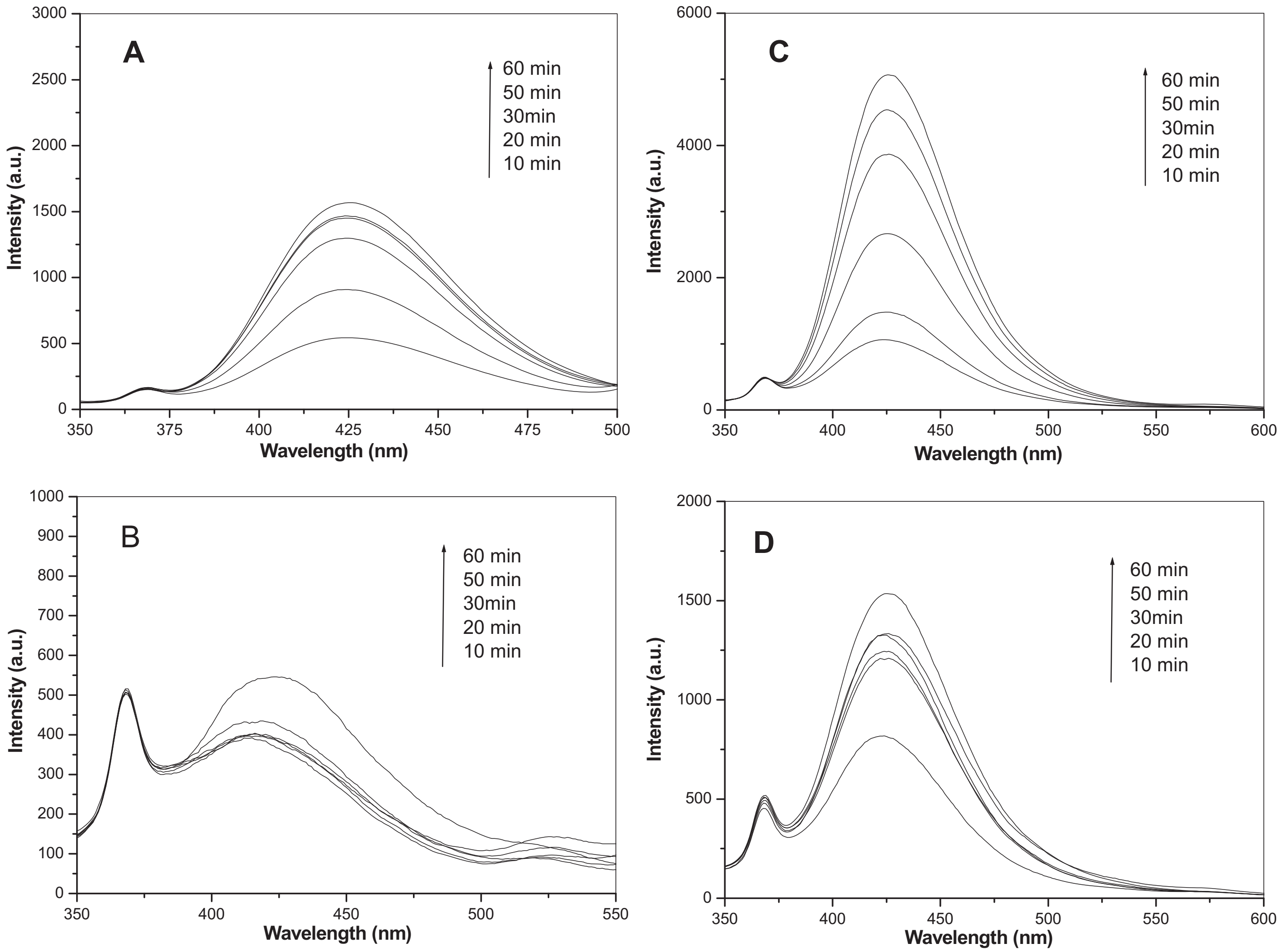

**Fig. 7.** The PL signal peaks of $^{\cdot}OH$ radicals at 425 nm in the presence of $AgPO_3$ microspheres. (A) with $AgPO_3$ (not air-bubbled); (B) without $AgPO_3$ (not air-bubbled); (C) with $O_2$ by air-bubbled (50 mL/min); (D) $H_2O_2$ (30 wt.%, 0.5 mL, not air-bubbled).

of $^{\cdot}OH$ radicals is too small to oxidize RhB molecules. It is reported that $O_2$ and $H_2O_2$ can promote the production of $^{\cdot}OH$ radicals in water under ultrasonic irradiation [10]. Therefore, to study the effect on the $^{\cdot}OH$ radicals concentration of $O_2$ and $H_2O_2$, the dependence of the $^{\cdot}OH$ radicals concentration on the $H_2O_2$ and $O_2$ over $AgPO_3$ microspheres is researched under the same experimental conditions. Fig. 7C (with $O_2$ by air-bubbled, 50 mL/min) and 7D (with $H_2O_2$, 30 wt.%, 0.5 mL) exhibits that the intensity of the PL emission peak at 425 nm increases rapidly with elapsed reaction time, indicating that the $^{\cdot}OH$ radical concentration in the system gradually increased. In Fig. 7C, the peak intensity of PL is the highest than those of Fig. 7, which shows that $O_2$ can greatly facilitate the generation of a large number of $^{\cdot}OH$ radicals over $AgPO_3$ microspheres under ultrasonic irradiation. In comparison with Fig. 7D and A, the PL intensity in Fig. 7D is stronger than that of Fig. 7A before 20 min, indicating that $H_2O_2$ is also able to increase the generation of $^{\cdot}OH$ radicals over $AgPO_3$ microspheres under ultrasonic irradiation. Base on the above experimental data and reference [10], the sonocatalytic mechanism of the $AgPO_3$ microspheres is proposed below:

$H_2O$ + ultrasound + $AgPO_3 \rightarrow {}^{\cdot}OH + {}^{\cdot}H$ (Fig. 7A)
$O_2$ (air-bubbles) + ultrasound + $AgPO_3 \rightarrow 2O^{\cdot} \rightarrow {}^{\cdot}O + H_2O \rightarrow 2{}^{\cdot}OH$ (Fig. 7C)
$O_2$ (air-bubbles) + $H^{\cdot} \rightarrow {}^{\cdot}O_2H \rightarrow H_2O_2 + O_2 \rightarrow H_2O_2$ + ultrasound + $AgPO_3 \rightarrow 2{}^{\cdot}OH$ (Fig. 7D)
${}^{\cdot}OH$ + RhB → small moleculars

## 4. Conclusion

In summary, $AgPO_3$ microspheres have been constructed via a one-step hydrothermal process. Moreover, RhB was more efficiently sonodegraded by the as-prepared $AgPO_3$ microspheres.

## References

[1] A.Z. Abdullah, P.Y. Ling, Heat treatment effects on the characteristics and sonocatalytic performance of $TiO_2$ in the degradation of organic dyes in aqueous solution, J. Hazard. Mater. 173 (2010) 159–167.
[2] P. Cui, Y.Z. Chen, G.J. Chen, Degradation of low concentration methyl orange in aqueous solution through sonophotocatalysis with simultaneous recovery of photocatalyst by ceramic membrane microfiltration, Ind. Eng. Chem. Res. 50 (2011) 3947–3954.
[3] A.K. Shriwas, P.R. Gogate, Intensification of degradation of 2,4,6-trichlorophenol using sonochemical reactors: understanding mechanism and scale-up aspects, Ind. Eng. Chem. Res. 50 (2011) 9601–9608.
[4] C. Balaji, V.S. Moholkar, A.B. Pandit, M. Ashokkumar, Mechanistic investigations on sonophotocatalytic degradation of textile dyes with surface active solutes, Ind. Eng. Chem. Res. 50 (2011) 11485–11494.

[5] Y.H. He, F. Grieser, M. Ashokkumar, Kinetics and mechanism for the sonophotocatalytic degradation of p-chlorobenzoic acid, J. Phys. Chem. A 115 (2011) 6582–6588.

[6] Z. Erena, N.H. Inceb, Sonolytic and sonocatalytic degradation of azo dyes by low and high frequency ultrasound, J. Hazard. Mater. 177 (2010) 1019–1024.

[7] J. Wang, T. Ma, Z.H. Zhang, X.D. Zhang, Y.F. Jiang, W. Sun, R.H. Li, P. Zhang, Investigation on the transition crystal of ordinary rutile $TiO_2$ powder by microwave irradiation in hydrogen peroxide solution and its sonocatalytic activity, Ultrason. Sonochem. 14 (2007) 575–582.

[8] M.H. Priya, G. Madras, Kinetics of $TiO_2$-catalyzed ultrasonic degradation of rhodamine dyes, Ind. Eng. Chem. Res. 45 (2006) 913–921.

[9] M. Kubo, K. Matsuoka, A. Takahashi, N. Shibasaki-Kitakawa, T. Yonemoto, Kinetics of ultrasonic degradation of phenol in the presence of $TiO_2$ particles, Ultrason. Sonochem. 12 (2005) 263–269.

[10] L. Zhao, J. Ma, X.D. Zhai, Synergetic effect of ultrasound with dual fields for the degradation of nitrobenzene in aqueous solution, Environ. Sci. Technol. 43 (2009) 5094–5099.